I&EC research
Industrial & Engineering Chemistry Research

Article

pubs.acs.org/IECR

Thermal-Responsive Block Copolymers for Surface with Reversible Switchable Wettability

Jin-Jin Li, Yin-Ning Zhou, and Zheng-Hong Luo*

Department of Chemical Engineering, School of Chemistry and Chemical Engineering, Shanghai Jiao Tong University, Shanghai 200240, P. R. China

Supporting Information

ABSTRACT: A series of thermal-responsive block copolymers, i.e., poly(methyl methacrylate)-*block*-poly(*N*-isopropylacrylamide) (PMMA-*b*-PNIPAAm), were successfully synthesized via successive copper(0)-mediated reversible-deactivation radical polymerization technology. Thermal properties of block copolymers with different PNIPAAm chain lengths were investigated by differential scanning calorimetery (DSC) and thermogravimetric analysis (TGA). The well-separated glass transition temperature values shown in DSC results indicate that two chemically different blocks, PNIPAAm and PMMA, are incompatible and phase-segregated. The thermal degradation results show that the thermal stability of these copolymers was improved through incorporating the PNIPAAm segments. The $PMMA_{120}$-*b*-$PNIPAAm_{86}$ and $PMMA_{120}$-*b*-$PNIPAAm_{130}$ maintain stability and undergo one-stage degradation when the temperature increases above 360 °C. Because of the synergistic effect of copolymer composition and copolymer film roughness, the obtained reversible thermal-responsive wettability for the resulting copolymer-modified surfaces is different, which is enhanced by incorporating more functional NIPAAm units. Specifically, the variations of the static water contact angle for the surfaces fabricated by $PMMA_{120}$-*b*-$PNIPAAm_{40}$, $PMMA_{120}$-*b*-$PNIPAAm_{54}$, $PMMA_{120}$-*b*-$PNIPAAm_{86}$, and $PMMA_{120}$-*b*-$PNIPAAm_{130}$ are 18.7, 20.4, 26.8, and 34.3°, respectively. In addition, all as-prepared surfaces present a stable reversible thermal-responsive wettability, which can be applied to coatings with temperature-controllable wettability as well as manipulation of liquids in microfluidic devices.

1. INTRODUCTION

Recently, smart surfaces have attracted considerable interest in both fundamental research and industry because of their variable surface properties toward external stimuli.[1−4] Because of the importance of the wetting properties of a surface, smart interfacial materials with switchable wettability induced by different environmental stimuli, including temperature, pH, electric field, and light irradiation, have been fabricated and investigated.[5−11] Among them, poly(*N*-isopropylacrylamide) (PNIPAAm) modified smart surfaces exhibit reversible wettability switching between hydrophilicity and hydrophobicity upon the external temperature below and above lower critical solution temperature (LCST),[12,13] which may have wide applications in different fields, such as biomedical sciences,[14−16] microfluidic devices,[17] chromatography,[18] etc.

Poly(methyl methacrylate) (PMMA) is one of the well-known industrial materials and has been widely used. PMMA films can be modified to achieve the controllable surface wettability via incorporating a second thermal-responsive functional monomer (e.g., *N*-isopropylacrylamide (NIPAAm)). Simultaneously, new properties introduced by the second monomer potentially extend the applications of the surfaces.[18−24] In turn, hydrophobic PMMA with high glass transition temperature (T_g) servers as the physical cross-link of hydrophilic PNIPAAm, enhancing the stability of copolymer films in moist environments.[25]

In recent years, reversible-deactivation radical polymerization (RDRP) techniques were developed as robust tools for preparing diblock and other multiblock copolymers.[26] In general, nitroxide-mediated polymerization (NMP),[27] atom-transfer radical polymerization (ATRP),[28,29] and reversible addition−fragmentation chain transfer (RAFT) polymerization are commonly used.[30] More recently, the Cu(0)-mediated RDRP process has attracted great attention because of the advance in ultrafast polymerization with small amounts of catalyst.[31,32] Percec and co-workers demonstrated that the polymerization system containing reductant (i.e., hydrazine, ascorbic acid) becomes more tolerant to the oxygen.[33] The versatility of this technique has been applied in different media such as DMSO,[34,35] water,[36] alcohols,[37] DMF,[38] and even in the biologically complex media.[39] Also exploiting this approach, Cu(0)-mediated RDRP of functional water-soluble acrylic and acrylamide monomers including poly(ethylene glycol) acrylate, *N*-isopropylacrylamide, and *N*,*N*-dimethylacrylamide was carried out successfully in a controlled manner.[40−43] In addition, Haddleton and co-workers prepared multiblock and diblock glycopolymers by Cu(0)-mediated RDRP and investigated their interactions and potential applications in cellular processes including recognition, binding, and signaling.[44,45]

Benefiting from the Cu(0)-mediated RDRP, a series of well-defined chain length block copolymers (PMMA-*b*-PNIPAAm) were synthesized in an oxygen-tolerant system, as shown in Scheme 1. Thermal properties were evaluated to confirm whether the resulted copolymers are appropriate to the preparation of smart surfaces. Reversible thermal-responsive

Received: September 12, 2014
Revised: November 3, 2014
Accepted: November 7, 2014
Published: November 7, 2014

dx.doi.org/10.1021/ie503610n | *Ind. Eng. Chem. Res.* 2014, 53, 18112−18120

Scheme 1. Synthetic Outline of PMMA-Br and PMMA-*b*-PNIPAAm

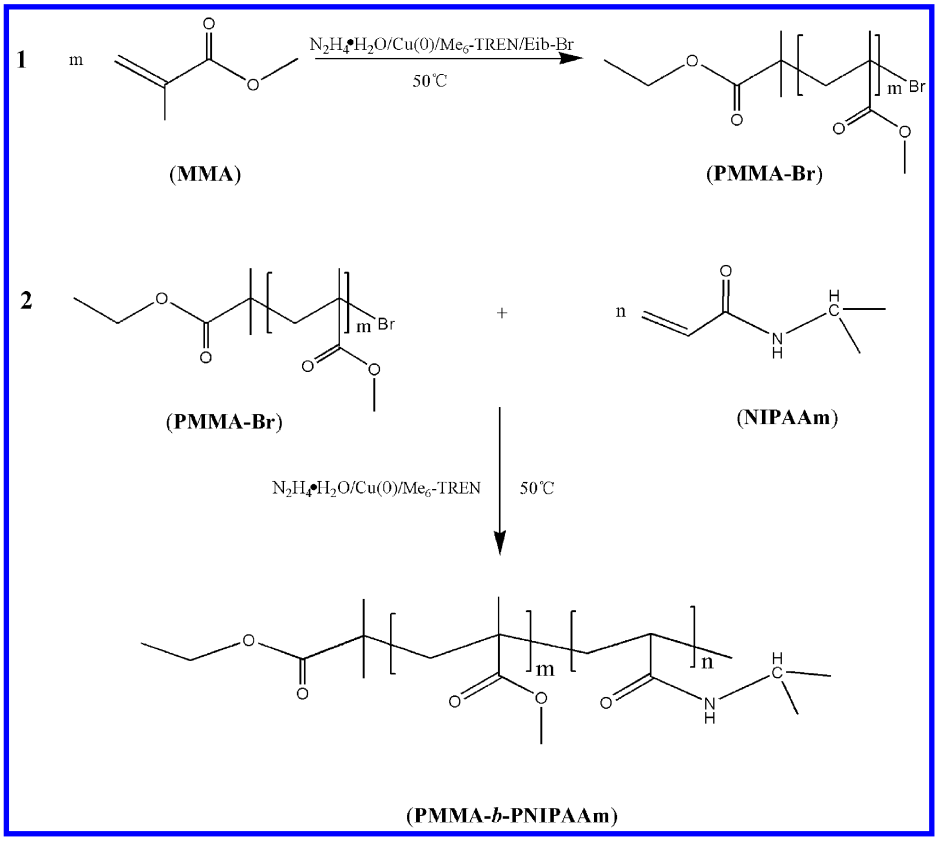

wettability of the resulting copolymer-modified surfaces is investigated by a temperature-controlled static water contact angle (SWCA) instrument at various temperatures. Particular attention is paid to the influences of volume fraction of PNIPAAm in the copolymers and surface morphologies on the thermal-responsive wettability of the block copolymer-modified surfaces.

2. MATERIALS AND METHODS

2.1. Materials. Methyl methacrylate (MMA, 99%, Sinopharm Chemical Reagent Co., Ltd. (SCRC)) was rinsed with 5 wt % aqueous NaOH solution to remove the inhibitor and dried with $MgSO_4$ overnight before use. *N*-Isopropylacrylamide (NIPAAm, 97%, TCI (Shanghai) Development Co., Ltd.) was recrystallized from a toluene/hexane solution (v/v = 1/2) and dried under vacuum prior to use. Ethyl 2-bromoisobutyrate (Eib-Br, 98%, Alfa Aesar), hexamethylated tris(2-aminothyl) amine (Me_6-TREN, 99%, Alfa Aesar), hydrazine monohydrate (N_2H_4·H_2O, 98%, TCI), and copper powder (Cu(0), 75 μm, 99%, Sigma-Aldrich) were used as received without further purification.

2.2. Synthesis of Macroinitiator PMMA-Br. MMA (5 mL, 47 mmol), DMF (5 mL), Cu(0) (15.04 mg, 0.235 mmol), N_2H_4·H_2O (11.2 μL, 0.235 mmol), and Me_6TREN (61.1 μL, 0.235 mmol) were first introduced into a 25 mL Schlenk flask and stirred for 15 min. Then, initiator Eib-Br (34.4 μL, 0.235 mmol) was added. The polymerization was carried out at 90 °C. The reaction mixture was diluted with $CHCl_3$ and passed through an Al_2O_3 column to remove the catalyst. Finally, the macroinitiator PMMA-Br was obtained by repeatedly pouring the concentrated solution into methanol and drying under vacuum at 40 °C.

2.3. Synthesis of PMMA-*b*-PNIPAAm Block Copolymers. Macroinitiator PMMA-Br (300 mg, 0.025 mmol), DMF/2-propanol mixed solvent (v/v% = 2/1, 3 mL), Cu(0) (1.6 mg, 0.025 mmol), N_2H_4·H_2O (1.2 μL, 0.025 mmol), and Me_6TREN (7.5 μL, 0.025 mmol) were first introduced into a 25 mL Schlenk flask and stirred for 5 min. Then, NIPAAm (565 mg, 5 mmol) dissolving in 1 mL of DMF/2-propanol mixed solution (v/v% = 2/1) was added to the flask. The polymerization was carried out at 50 °C for a predetermined time. After the catalyst was removed, PMMA-*b*-NIPAAm block copolymer was repeatedly precipitated from anhydrous ethyl ether and dried under vacuum at 40 °C.

2.4. Preparation of Copolymer Films. The polymer solution (3 wt % in THF) was spin-casted onto clean silicon wafer at 3000 rpm for 30 s and dried naturally for 24 h. Prior to modification, the silicon wafers were cleaned in a mixed solution with 10% HCl and KF for 10 min to remove the contamination. Then they were sonicated in acetone, ethyl alcohol, and deionized water separately for 30 min, followed by being dried with a nitrogen stream.

2.5. Measurements. *^{1}H NMR.* The compositions of copolymers were determined by nuclear magnetic resonance (^{1}H NMR) spectroscopy (Varian Mercury plus 400, 400 MHz) in $CDCl_3$ with tetramethylsilane (TMS) as internal standard.

FT-IR. Fourier-transform infrared (FT-IR) spectra were obtained on an Avatar 360 FTIR spectrophotometer by dispersing samples in KBr disks.

GPC. Molecular weights and molecular weight distributions (M_w/M_n) of polymers were determined on a gel permeation chromatograph (GPC, Tosoh Corporation) equipped with two HLC-8320 columns (TSK gel Super AWM-H; pore size, 9 μm; 6 × 150 mm, Tosoh Corporation) and a double-path, double-

dx.doi.org/10.1021/ie503610n | *Ind. Eng. Chem. Res.* 2014, 53, 18112−18120

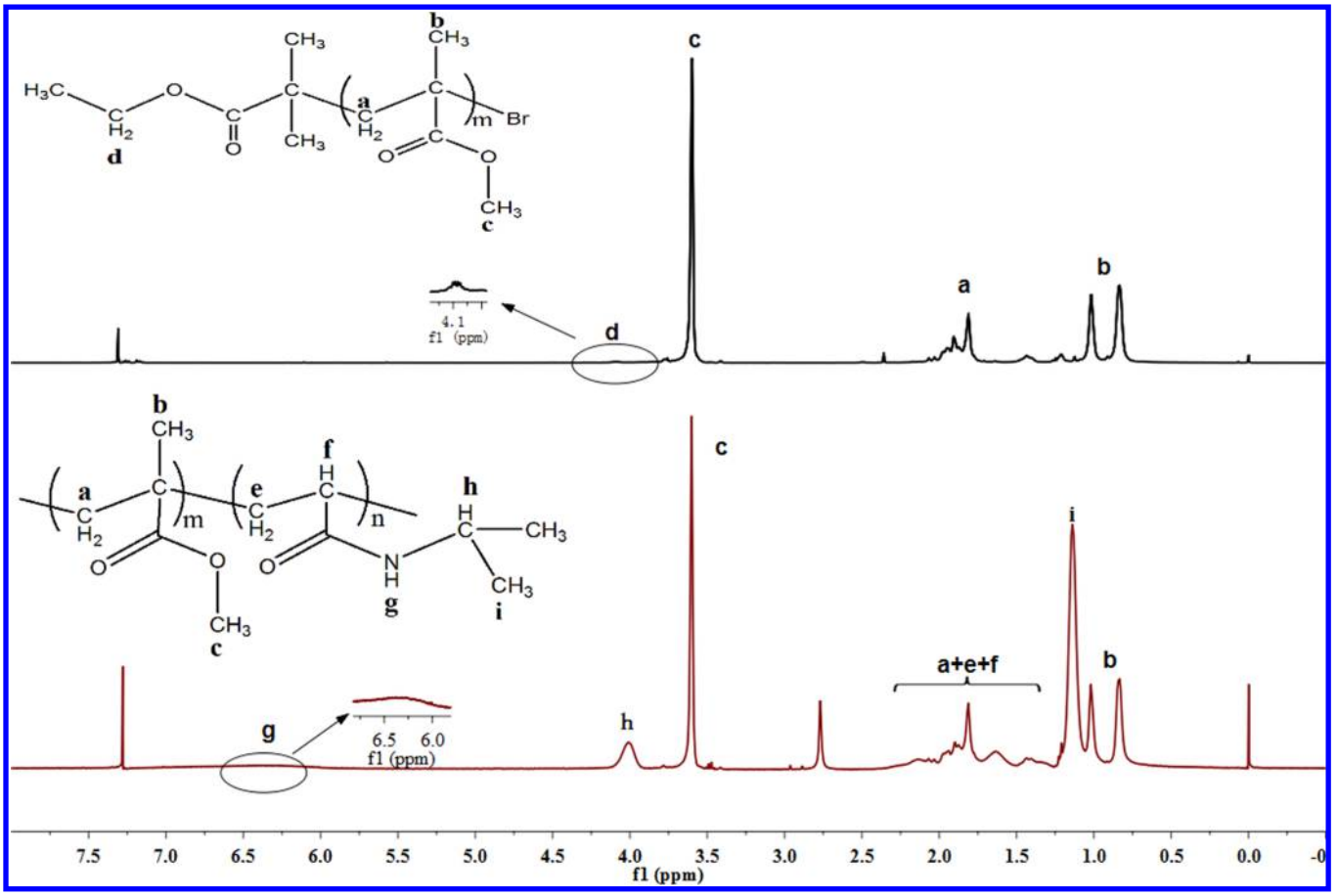

Figure 1. ^{1}H NMR spectra of (top spectrum) $PMMA_{120}$-Br and (bottom spectrum) $PMMA_{120}$-*b*-$PNIPAAm_{130}$.

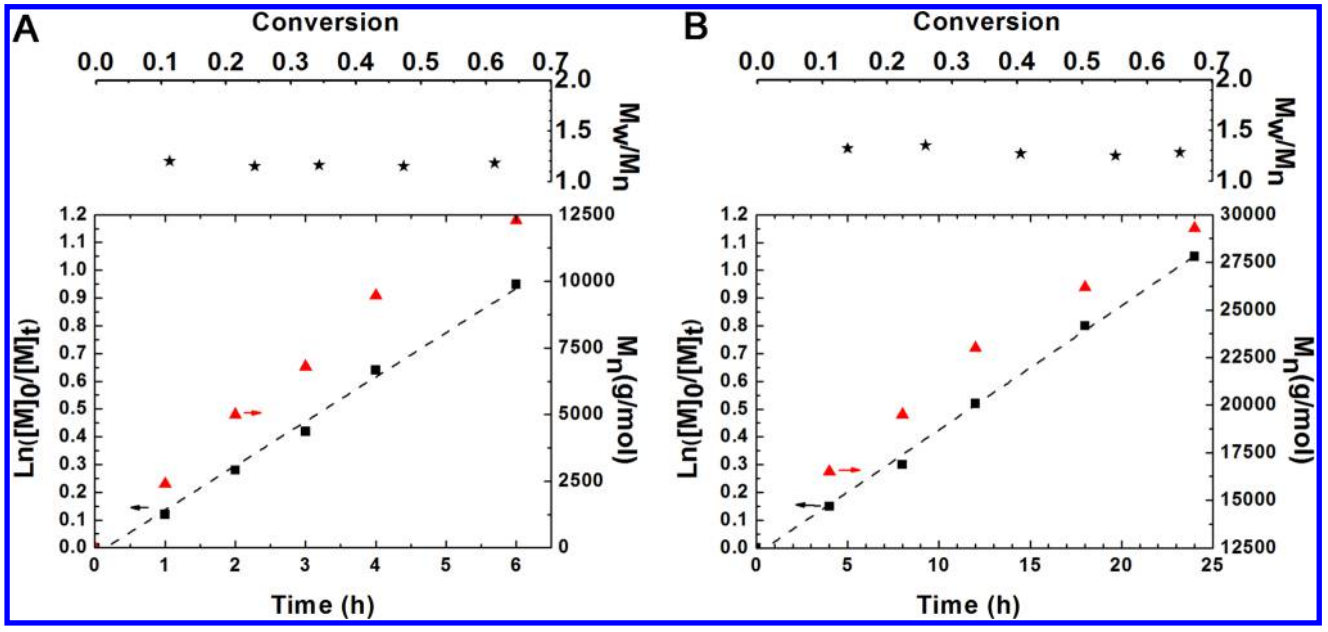

Figure 2. Kinetic plot and evolution of M_n and M_w/M_n for the synthesis of (A) $PMMA_{120}$-Br and (B) $PMMA_{120}$-*b*-$PNIPAAm_{130}$.

flow refractive index detector (Bryce) at 30 °C. The elution phase was DMF (0.01 mol/L LiBr; elution rate, 0.6 mL/min), and a series of poly methyl methacrylate (PMMA) was used as the conventional calibration standard.

TGA. Thermogravimetric analysis (TGA) was conducted on a Q5000 thermal gravimetric analyzer under a heating rate of 20 °C/min from room temperature to 800 °C in a nitrogen gas atmosphere.

DSC. The thermal analysis of the copolymers was carried out using a differential scanning calorimetery instrument (DSC; TA Instruments Q2000) under a dry nitrogen atmosphere. Dry nitrogen was purged into the DSC cell at a flow rate of 50 mL/

dx.doi.org/10.1021/ie503610n | *Ind. Eng. Chem. Res.* 2014, 53, 18112−18120

Table 1. Synthesis of PMMA-*b*-PNIPAAm by Cu(0)-Mediated RDRP[a]

no.	copolymer	time (h)	conv. (%)	M_n[a] (g/mol) (theo.)	M_n (g/mol) (GPC)	M_w/M_n (GPC)	f[b]
1	$PMMA_{120}$-*b*-$PNIPAAM_{40}$	6	20.0	16 540	18 100	1.31	0.24
2	$PMMA_{120}$-*b*-$PNIPAAM_{54}$	8	27.0	18 125	19 400	1.30	0.30
3	$PMMA_{120}$-*b*-$PNIPAAM_{86}$	14	43.0	21 745	23 500	1.26	0.41
4	$PMMA_{120}$-*b*-$PNIPAAM_{130}$	24	65.0	26 725	29 300	1.28	0.51

[a]Temperature = 50 °C; V_{sol} = DMF/2-propanol mixed solvent (v/v% = 2/1); $[NIPAAm]_0/[PMMA\text{-}Br]_0/[Cu(0)]_0/[N_2H_4{\cdot}H_2O]/[Me_6TREN]$ = 200/1/1/1/1; M_n (theo.) = ($[NIPAAm]_0/[Initiator]_0$) × conv. × 113.16 + 12 014. [b]The volume fraction of PNIPAAm, as the known densities of PNIPAAm and PMMA are 1.39 and 1.18 g cm^{-3}, respectively.

min. The samples were first heated at a rate of 10 °C/min from 0 to 200 °C and held at 200 °C for 5 min to eliminate thermal history. The samples were then cooled to 0 °C before being reheated to 200 °C at a rate of 10 °C/min. All data associated with the glass transition measurements were obtained from the second heating scan and taken as the midpoint of heat capacity change.

AFM. Surface morphology and roughness of spin-coated films were acquired on a Nanonavi E-Sweep (SII, Japan) atomic force microscopy (AFM) instrument in the tapping mode at room temperature.

SWCA. The static water contact angle of silicon surfaces functionalized by block copolymers was measured on a contact angle measuring instrument (KRUSS, DSA30) at the temperatures of 20, 25, 30, 35, 40, 45, and 50 °C by using the sessile drop method. The temperature was controlled by a TC40-MK2 temperature controller. A deionized water droplet (5 μL) was dropped onto the samples, which were blow-dried with N_2 and kept at the required temperature for 10 min.

3. RESULTS AND DISCUSSION

3.1. Characterization of Block Copolymers. Cu(0)-mediated RDRP was utilized to prepare PMMA-*b*-PNIPAAm copolymers because of the moderate polymerization condition and perfect end-functionality.[31−33] In the present work, the addition of reductant (hydrazine hydrate) makes the polymerization proceed in a system without strict deoxygenization. During reaction, Cu(0) can be oxidized to Cu_2O, but it can be reduced to Cu(0) again by hydrazine hydrate. Additionally, the Cu(II) complexes presented during polymerization can be reduced to the corresponding Cu(I) complexes by the excess reductant. This advantage indicates the approach has bright prospects in industrial polymerization engineering, in which moderate conditions and high efficiency are required.

The macroinitiator PMMA-Br was confirmed by ^{1}H NMR in Figure 1 (top spectrum). The characteristic peaks for the methyl ester protons of PMMA (3.60 ppm, 3H, $-OCH_3$) and the methylene protons of initiator (4.10 ppm, 2H, $-OCH_2CH_3$) were used to calculate the degree of polymerization (DP_n), which is 120. The M_n of PMMA-Br measured by GPC (Figure S1 in Supporting Information) is 13 200 g/mol, coinciding with the calculated value (M_n = 12 014 g/mol) within allowable error. Figure 2A shows the kinetic plot for the polymerization of MMA. There is an induction period within 1 h, which is attributed to the Cu_2O reduction. After that, polymerization follows pseudo-first-order kinetics, indicating the nearly constant concentration of radical in this system during reaction. In addition, the approximately linear increase in M_n with time and M_w/M_n of PMMA-Br (1.15−1.20) demonstrate that Cu(0)-RDRP is of well-controlled and "living" feature under an oxygen-tolerant system.

The block copolymer PMMA-*b*-PNIPAAm prepared via chain extension of PMMA-Br with NIPAAm was verified by the appearance of characteristic peaks at 4.0 and 6.0−7.0 ppm corresponding to the methine proton of isopropyl groups and the amide proton next to the isopropyl groups, respectively, in Figure 1 (bottom spectrum). The peak area ratio of PNIPAAm (4.0 ppm, 1H, $-NH-$) and PMMA (3.6 ppm, 3H, $-OCH_3$) indicates that the unit number of NIPAAm is 130. The M_n of $PMMA_{120}$-*b*-$PNIPAAm_{130}$ is 26 700 g/mol by calculation and is 29 300 g/mol by GPC (Figure S1 in Supporting Information). The similar kinetic behavior of polymerization can also be found in Figure 2B. However, there is a relatively broader M_w/M_n (1.25−1.32) for PMMA-*b*-PNIPAAm, which may result from the irreversible termination favored by high radical concentration in DMF/2-propanol mixed solvent.

According to the kinetics study, block copolymers with different DP_n of PNIPAAm can be obtained by controlling the reaction time. The detailed experimental conditions for the four block copolymers are given in Table 1. The compositions of resulting copolymers were analyzed by ^{1}H NMR and FT-IR (Figures S2 and S3 in Supporting Information). In addition, Figure S1 demonstrates the GPC traces recorded for all resulting polymers, and the results are listed in Table 1.

3.2. Thermal Properties. Block copolymers produced through covalently connecting two chemically different polymers at a single point can form nanostructures with separation. The separated domains exhibit properties of corresponding blocks independently and also affect each other.[25] To confirm whether the resulting copolymers are appropriate candidate materials for the preparation of smart surfaces, the thermal behaviors of block copolymers were studied by using DSC (Figure 3) and TGA (Figure 4).

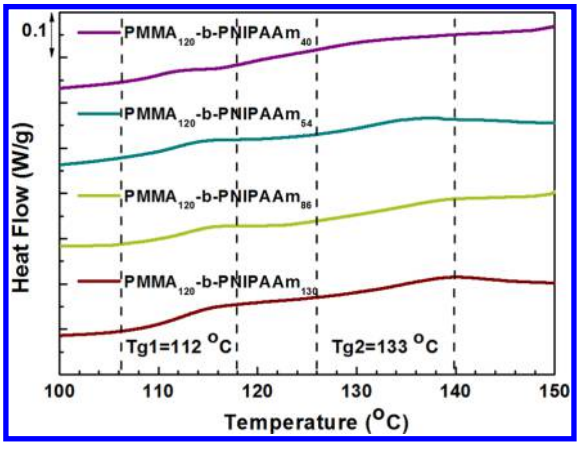

Figure 3. DSC curves of $PMMA_{120}$-*b*-$PNIPAAm_n$ (n = 40, 54, 86, 130).

dx.doi.org/10.1021/ie503610n | Ind. Eng. Chem. Res. 2014, 53, 18112−18120

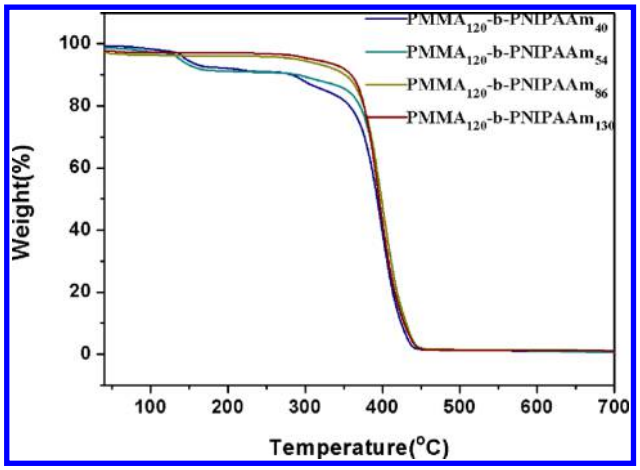

Figure 4. TGA curves of PMMA$_{120}$-*b*-PNIPAAm$_n$ (n = 40, 54, 86, 130).

Glass transition temperature (T_g) of PMMA or PNIPAAm is not a definite value, which varies in some ranges and mainly depends on the factors of tacticity, molecular weight, and water sorption.[48−54] Cu(0)-mediated RDRP as a radical polymerization enables the synthesis of polymers having controlled molecular weights,[52−54] whereas the stereostructure of polymers cannot be controlled in common conditions. Therefore, the resulting PMMA-*b*-PNIPAAm block copolymers contain atactic PMMA block with a classic T_g at about 105 °C[50] and atactic PNIPAAm block with a classic T_g at about 130 °C.[52] In Figure 3, two discernible T_g values are observed in the DSC heating curves of the block copolymers with different fractions of PNIPAAm. The first T_g at about 112 °C related to the PMMA segment is higher than 105 °C, which is likely due to the effect of hydrogen bonding in NIPAAm and the cooperation between PMMA and PNIPAAm blocks. The second T_g performed at 133 °C related to PNIPAAm block agrees with the T_g (∼130 °C) of PNIPAAm homopolymer. These well-separated T_g values indicate that two chemically different blocks, PNIPAAm and PMMA, are incompatible and phase-segregated, which has an effect on the wettability of the surface.

Kashiwagi et al.[46] demonstrated that free radically polymerized PMMA undergoes a three-step degradation. The first one at lower temperature (around 165 °C) is attributed to the scissions of head-to-head linkages (H−H); the second stage at ∼270 °C is associated with end-initiated depolymerization from the unsaturated vinyl ends; the third stage at ∼360 °C is due to random scissions within the polymer chain. By contrast, PNIPAAm degrades in a single step around 330−440 °C because of the degradation of the backbone chain.[47] Thermograms in Figure 4 indicate that the degradation behavior of the resulting block copolymers has been influenced by both PMMA and PNIPAAm blocks. The degradation behaviors of PMMA$_{120}$-*b*-PNIPAAm$_{40}$ and PMMA$_{120}$-*b*-PNIPAAm$_{54}$ with a lower volume fraction of PNIPAAm are close to PMMA; the degradation around 130−170 °C associated with scissions of head-to-head linkages (H−H) and the stage ∼280−330 °C associated with scissions at unsaturated vinyl chain ends are clearly observed. The mass loss rates at the third stages are higher for the block copolymers compared to that of the macroinitiator PMMA-Br possibly because the degradation of the backbone chain of PNIPAAm block also occurs around this temperature. As the length of PNIPAAm increase, the nature of copolymers is gradually approaching to PNIPAAm. PMMA$_{120}$-*b*-PNIPAAm$_{86}$ and PMMA$_{120}$-*b*-PNIPAAm$_{130}$ maintain stability in a certain scope of temperatures and undergo one-stage degradation when the temperature increases above 360 °C; the mass loss rates above 360 °C become higher because the degradation of the backbone chain of both PNIPAAm block and PMMA block all occur around this temperature. All the block copolymers yield a small amount of residual mass (<5%) as temperature increase to 700 °C. These thermal degradation results indicate that the thermal stability of these copolymers was improved through incorporating the PNIPAAm segments. Especially block copolymers with a higher volume fraction of PNIPAAm are confirmed with a good thermal stability, which can be used to prepare smart surfaces using a high-temperature environment.

3.3. Reversible Thermal-Responsive Surface Wettability. PNIPAAm is an extensively studied thermal-responsive polymer, which undergoes a phase transition from hydrophilic dissolved state to hydrophobic aggregation regulated by temperature in the aqueous circumstance.[12,55] Thus, the water-soluble PNIPAAm homopolymer will become an amorphous form at wetted surface, which is unsuitable for coating applications. The incorporation of PMMA segment into PNIPAAm-based block copolymer can not only significantly improve the strength of such functional coating but also result in the surface having a transition from hydrophilic to hydrophobic below or above LCST.

Herein, silicon wafers were modified by resulting block copolymers with different PNIPAAm chain fractions, and the influence of PNIPAAm blocks on the thermal-responsive behavior of surfaces was investigated using temperature-controlled SWCA measurement from 20 to 50 °C. Results in Figure 5 show that the SWCA increases with the increase of temperature in all the cases. As for the surfaces fabricated by PMMA$_{120}$-*b*-PNIPAAm$_{40}$ and PMMA$_{120}$-*b*-PNIPAAm$_{54}$ with shorter PNIPAAm segments, the values of WCA increase gradually from 67.2 to 85.9° and from 66.2 to 86.6°, respectively. It is interesting that SWCA values of both the surfaces fabricated by PMMA$_{120}$-*b*-PNIPAAm$_{86}$ and PMMA$_{120}$-

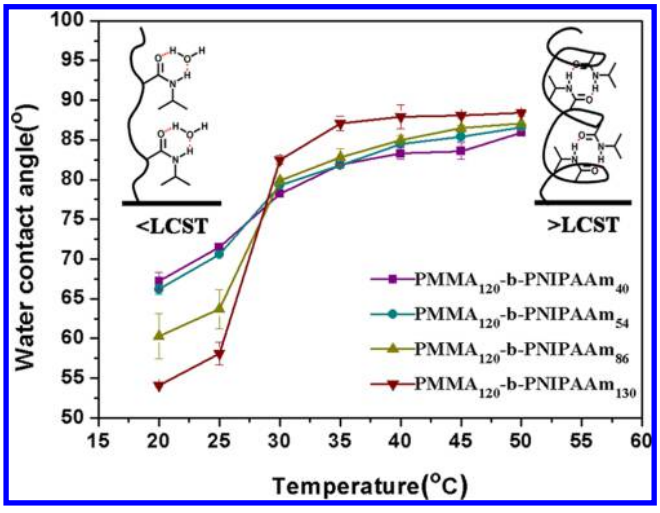

Figure 5. Temperature dependences of static WCA for the surfaces modified by PMMA$_{120}$-*b*-PNIPAAm$_n$ (n = 40, 54, 86, 130). The insets are schematic representations of the intermolecular and intramolecular hydrogen bonding interaction for the transformation of hydrophilicity and hydrophobicity.

dx.doi.org/10.1021/ie503610n | Ind. Eng. Chem. Res. 2014, 53, 18112−18120

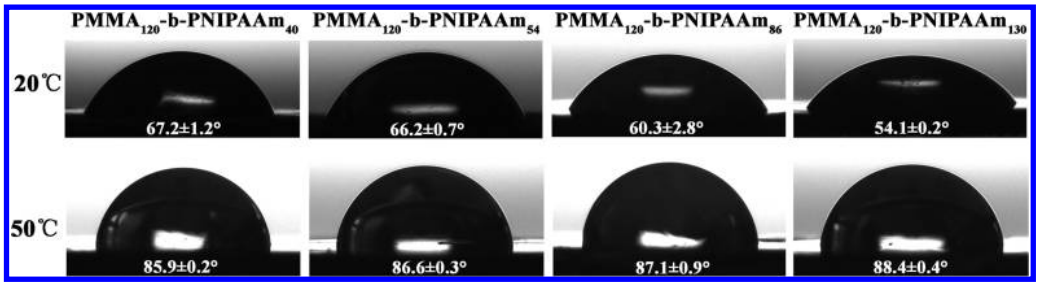

Figure 6. Static WCA images of surfaces modified by $PMMA_{120}$-*b*-$PNIPAAm_n$ (n = 40, 54, 86, 130) at 20 and 50 °C.

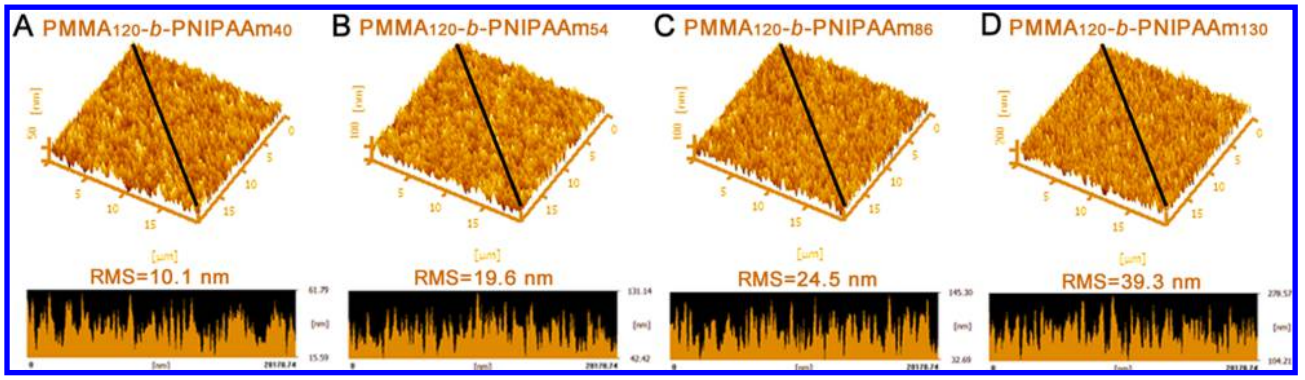

Figure 7. AFM 3D height images, global root-mean-square roughness (RMS), and corresponding section (black line) profiles of surfaces modified by $PMMA_{120}$-*b*-$PNIPAAm_n$ (n = 40, 54, 86, 130) in 20 μm scale.

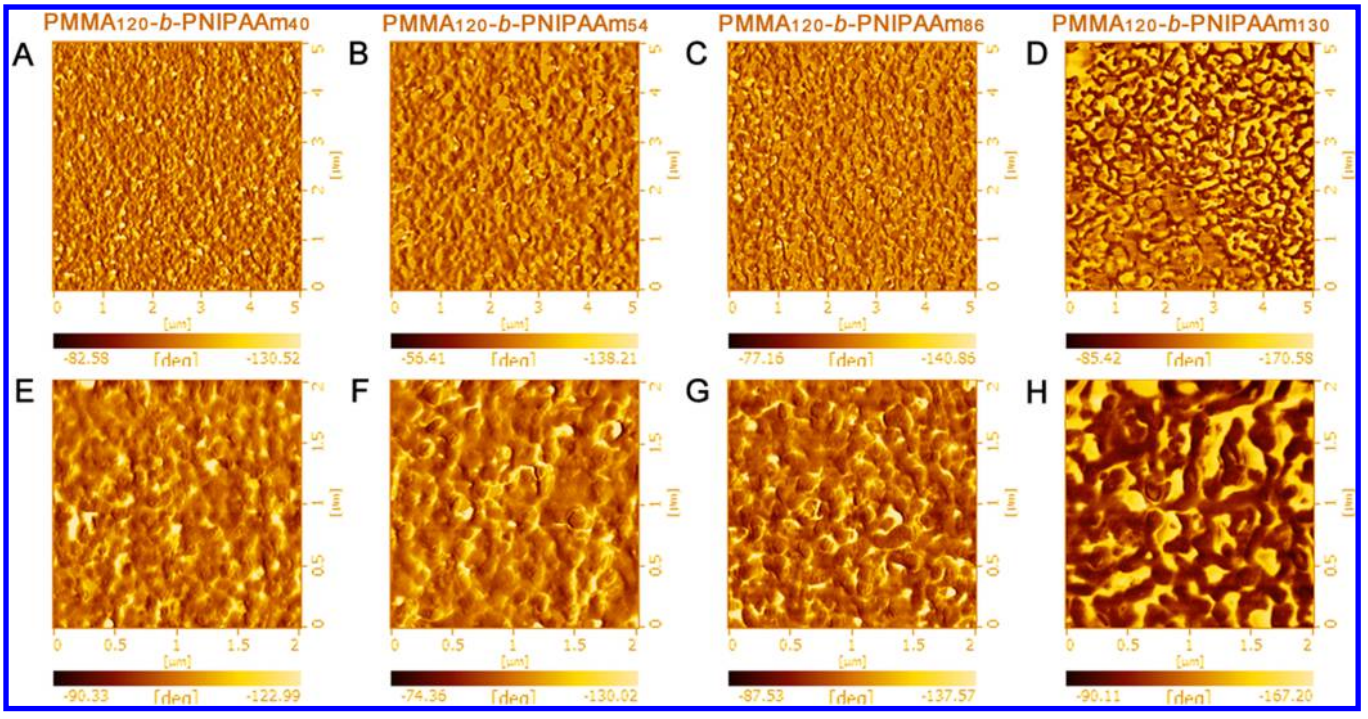

Figure 8. AFM phase images (panels A–D in 5 μm scale, and panels E–H in 2 μm scale) of surfaces modified by $PMMA_{120}$-*b*-$PNIPAAm_n$ (n = 40, 54, 86, 130).

b-$PNIPAAm_{130}$ experience a gradual increase with the increase of temperature (from 20 to 25 °C), followed by a sharp increase in the 25–35 °C temperature range. The SWCA changes from 60.3 to 87.1° for the former and from about 54.1 to 88.4° for the latter. Both the variations (ΔSWCA = 27° and 34°) are larger than those (ΔSWCA = 20°) of surfaces modified by copolymers with lower thermal-responsive PNIPAAm content. The representative SWCA images at 20 and 50 °C presented in Figure 6 clearly show that the surfaces modified by copolymers have a temperature tunable wettability. The different controllable wettability of functional silicon surface would result from the synergistic effects of copolymer composition and roughness. It is notable that the initial SWCA values are varied for different block copolymers, which is attributed to the effect of surface composition. The higher the PNIPAAm fraction is, the more sites for hydrogen bonding

dx.doi.org/10.1021/ie503610n | *Ind. Eng. Chem. Res.* 2014, 53, 18112–18120

with water molecules (H_2O), that is, the hydrophility of the surface is enhanced. However, all the SWCA values reach a similar stable level at above LCST, which is limited by an essential property of the functional copolymer film.

These intriguing results related to the temperature sensitivity of PNIPAAm segments might be caused by the formation of intermolecular or intramolecular hydrogen bonds, as graphically demonstrated in the insets of Figure 5.[55] The intermolecular hydrogen bonding between C═O/N−H groups and H_2O predominates below the LCST. The hydrated and swollen PNIPAAm chains promote the hydrophilicity of surfaces. As temperature increases above the LCST, the intramolecular hydrogen bonds formed between C═O and N−H groups lead to the collapse and dehydration of PNIPAAm chains. Thus, the surfaces exhibit relative hydrophobicity at high temperatures.

On the other hand, roughness also has an impact on the surface wettability. The different volume fractions of PNIPAAm involved in copolymer films lead to various surface roughnesses, which might be another reason for the different SWCA variations (ΔSWCA). AFM was used to detect the surface morphologies and morphological differences among four block copolymers films at 20 °C, as illustrated in Figures 7 and 8. The global root-mean-square (RMS) roughness provided by the AFM 3D height images are about 10.1, 19.6, 24.5, and 39.3 nm, which correspond to four different block copolymers (Figure 7A−D). The surface roughness increases by increasing the volume fraction of PNIPAAm, which might result from the different level of phase separation and solvent-binding ability. Additionally, all the surfaces with uniform micro- and nanostructures are illustrated by the corresponding section profiles in the bottom of Figure 7. As shown in Figure 8A−D, the inhomogeneity degree of as-prepared films becomes more apparent as the PNIPAAm block length increases. In Figure 8E−H, one can find the distinctive domains for PMMA and PNIPAAm on the four surfaces at the 2 μm scale, where the brighter areas in the phase images are recognized as PNIPAAm.[25] Obviously, the surface area is gradually occupied by PNIPAAm domains as the volume fraction of PNIPAAm increases. These results confirm that all block copolymers form rough structures on the surface, which might result from the enhanced incompatibility of both blocks caused by increasing volume fraction. The improved roughness of as-fabricated surfaces is supposed to have a synergistic effect with chemical composition on the different wetting ability.

Herein, the surface asperities consist of as-prepared polymeric materials; the water drop below LCST soaks into the grooves. This phenomenon is speculated to be in accord with the Wenzel model. The Wenzel model is a classical hypothesis explaining the wettability of a rough surface which considers the rough surface to be wetted by water drop, therefore leading to the increase of liquid−soild interfacial area. The fact is that the hydrophilicity of hydrophilic surfaces ($\theta < 90°$) will be enhanced, and hyrdrophobic surfaces ($\theta > 90°$) become more hydrophobic as the roughness increases.[56] The relationship between the contact angle (θ_r) on a rough surface and the Young's contact angle (θ_Y) on a flat surface in the Wenzel model is expressed as $\cos \theta_r = r \cos \theta_Y$, where r, roughness factor, is obtained by dividing the actual area by the geometric area of wetted surface (r is larger than 1). If the roughness of examined surface increases, r would become larger, hence leading to the further decrease of θ_r. Our experimental phenomenon that the hydrophility of the functional surface increases as the surface roughness increases can be thought of as the fact that the copolymer composition plays the predominant role and roughness intensifies the wetting controllability.

The reversibility of as-prepared surfaces is important for their application. As presented in Figure 9, all the functional surfaces

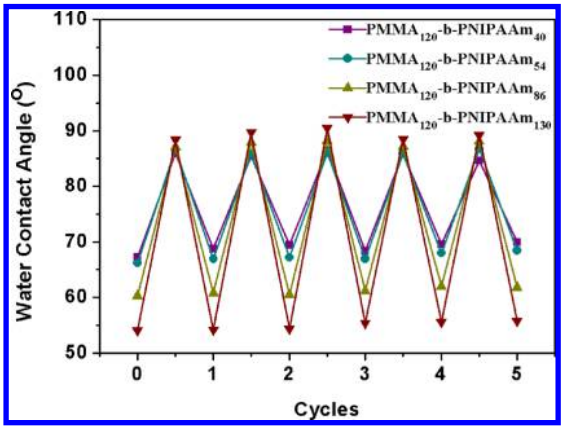

Figure 9. Reversible static WCA transition of the surfaces modified by $PMMA_{120}$-*b*-$PNIPAAm_n$ (n = 40, 54, 86, 130) between 20 °C (<LCST) and 50 °C (>LCST).

demonstrate reversible thermal-responsive wettability and good stability by adjusting the applied temperature below and above LCST of PNIPAAm. Compared with the traditional industrial polymers, this unique alternative product can control the spread of liquids on a surface, which has an application in microanalytical devices.

4. CONCLUSION

In this work, a series of thermal-responsive block copolymers, PMMA-*b*-PNIPAAm, were successfully synthesized via sequential Cu(0)-mediated RDRP in an oxygen-tolerant system. Kinetics study showed that this technique ensures the preparation of copolymers with well-defined chain length and narrow molecular weight distribution. The composition of resulting copolymers was confirmed by ^{1}H NMR and FT-IR. All block copolymers show two discernible T_g values in DSC curves, indicating that two chemically different blocks PNIPAAm and PMMA are incompatible and phase-segregated, which has an effect on the wettability of the surface. TGA analysis showed that these block copolymers have good thermal stability, which can be used to prepare smart surfaces for use in high-temperature environments.

The reversible thermal-responsive surfaces with temperature-tunable wettability were demonstrated by SWCA. Specifically, the variations of SWCA for the surfaces fabricated by $PMMA_{120}$-*b*-$PNIPAAm_{40}$, $PMMA_{120}$-*b*-$PNIPAAm_{54}$, $PMMA_{120}$-*b*-$PNIPAAm_{86}$, and $PMMA_{120}$-*b*-$PNIPAAm_{130}$ are 18.7, 20.4, 26.8, and 34.3°, respectively. Further studies conducted by AFM illustrated the effect of volume fraction of PNIPAAm on the morphology of as-fabricated smart surfaces. The RMS roughness obtained from the AFM 3D height images are about 10.1, 19.6, 24.5, and 39.3 nm, which correspond to the four different block copolymers, respectively. The different controllable wettability of functional silicon surfaces result from the synergistic effects of copolymer composition and copolymer film roughness.

Finally, the reversible performance of all copolymer films remains well after five temperature switching cycles. Overall,

the as-prepared smart surfaces modified by functional copolymer can be used in applications requiring coating with temperature-controllable wettability as well as manipulation of liquids in microfluidic devices.

■ ASSOCIATED CONTENT

Supporting Information

More characterization of the copolymers with different PNIPAAm block length (i.e., ^{1}H NMR, FT-IR, and GPC figures). This material is available free of charge via the Internet at http://pubs.acs.org.

■ AUTHOR INFORMATION

Corresponding Author

*E-mail: luozh@sjtu.edu.cn. Tel.: +86-21-54745602. Fax: +86-21-54745602.

Notes

The authors declare no competing financial interest.

■ ACKNOWLEDGMENTS

The authors thank the National Natural Science Foundation of China (21276213), the Research Fund for the Doctoral Program of Higher Education (20130073110077), and the National High Technology Research and Development Program of China (2013AA032302) for supporting this work.

■ REFERENCES

(1) Xia, F.; Zhu, Y.; Feng, L.; Jiang, L. Smart Responsive Surfaces Switching Reversibly Between Super-Hydrophobicity and Super-Hydrophilicity. *Soft Matter* **2009**, *5*, 275−281.

(2) Win, B. W.; Hao, J. C. Reversibly Switchable Wettability. *Chem. Soc. Rev.* **2010**, *39*, 769−782.

(3) Karimian, N.; Zavar, M. H. A.; Chamsaz, M.; Turner, A. P. F.; Tiwari, A. On/off-Switchable Electrochemical Folic Acid Sensor Based on Molecularly Imprinted Polymer Electrode. *Electrochem. Commun.* **2013**, *36*, 92−95.

(4) Ashutosh Tiwari, A.; Kobayashi, H. *Responsive Material and Methods: State-of-the-Art Stimuli-Responsive Materials and Their Applications*; Wiley: Hoboken, NJ, 2013.

(5) Shi, X. J.; Chen, G. J.; Wang, Y. W.; Yuan, L.; Zhang, Q.; Haddleton, D. M.; Chen, H. Control the Wettability of Poly(*N*-isopropylacrylamide-*co*-1-adamantan-1-ylmethyl acrylate) Modified Surfaces: The More Ada, the Bigger Impact? *Langmuir* **2013**, *29*, 14188−14195.

(6) Whitesides, G. M.; Laibinis, P. E. Wet Chemical Approaches to the Characterization of Organic Surfaces: Self-Assembled Monolayers, Wetting, and the Physical-Organic Chemistry of the Solid-Liquid Interface. *Langmuir* **1990**, *6*, 87−96.

(7) Li, S. J.; Ge, Y.; Tiwari, A.; Wang, S. Q.; Turner, A. P. F.; Piletsky, S. A. 'On/off'-Switchable Catalysis by a Smart Enzyme-like Imprinted Polymer. *J. Catal.* **2011**, *278*, 173−180.

(8) Wang, S.; Feng, X.; Yao, J.; Jiang, L. Controlling Wettability and Photochromism in a Dual-Responsive Tungsten Oxide Film. *Angew. Chem., Int. Ed.* **2006**, *45*, 1264−1267.

(9) Bai, H.; Tian, X.; Zheng, Y.; Ju, J.; Zhao, Y.; Jiang, L. Direction Controlled Driving of Tiny Water Drops on Bioinspired Artificial Spider Silks. *Adv. Mater. (Weinheim, Ger.)* **2010**, *22*, 5521−5525.

(10) Abrakhi, S.; Péralta, S.; Fichet, O.; Teyssié, D.; Cantin, S. Poly(azobenzene acrylate-*co*-fluorinated acrylate) Spin-Coated Films: Influence of the Composition on the Photo-Controlled Wettability. *Langmuir* **2013**, *29*, 9499−9509.

(11) Zhou, Y.-N.; Li, J.-J.; Zhang, Q.; Luo, Z.-H. A Novel Fluorinated Polymeric Product for Photoreversibly Switchable Hydrophobic Surface. *AIChE J.* **2014**, DOI: 10.1002/aic.14602.

(12) Schild, H. G. Poly(*N*-isopropylacrylamide): Experiment, Theory and Application. *Prog. Polym. Sci.* **1992**, *17*, 163−249.

(13) Hu, Z.; Chen, Y.; Wang, C.; Zheng, Y.; Li, Y. Polymer Gels with Engineered Environmentally Responsive Surface Patterns. *Nature (London, U.K.)* **1998**, *393*, 149−152.

(14) Tang, Z.; Akiyama, Y.; Okano, T. Temperature-Responsive Polymer Modified Surface for Cell Sheet Engineering. *Polymers* **2012**, *4*, 1478−1498.

(15) Parlak, O.; Turner, A. P. F.; Tiwari, A. On/off-Switchable Zipper-Like Bioelectronics on a Graphene Interface. *Adv. Mater. (Weinheim, Ger.)* **2014**, *26*, 482−486.

(16) Liu, H.; Liu, X.; Meng, J.; Zhang, P.; Yang, G.; Su, B.; Sun, K.; Chen, L.; Han, D.; Wang, S.; Jiang, L. Hydrophobic Interaction-Mediated Capture and Release of Cancer Cells on Thermoresponsive Nanostructured Surfaces. *Adv. Mater. (Weinheim, Ger.)* **2013**, *25*, 922−927.

(17) Hou, X.; Yang, F.; Li, L.; Song, Y.; Jiang, L.; Zhu, D. A Biomimetic Asymmetric Responsive Single Nanochannel. *J. Am. Chem. Soc.* **2010**, *132*, 11736−11742.

(18) Kanazawa, H.; Okano, T. Temperature-Responsive Chromatography for the Separation of Biomolecules. *J. Chromatogr., A* **2011**, *1218*, 8738−8747.

(19) Sun, T.; Qing, G. Biomimetic Smart Interface Materials for Biological Applications. *Adv. Mater. (Weinheim, Ger.)* **2011**, *23*, H57−H77.

(20) Mendes, P. M. Stimuli-Responsive Surfaces for Bio-Applications. *Chem. Soc. Rev.* **2008**, *37*, 2512−2529.

(21) Yu, Q.; Zhang, Y. X.; Chen, H.; Zhou, F.; Wu, Z. Q.; Huang, H.; Brash, J. L. Protein Adsorption and Cell Adhesion/Detachment Behavior on Dual-Responsive Silicon Surfaces Modified with Poly(*N*-isopropylacrylamide)-*block*-polystyrene Copolymer. *Langmuir* **2010**, *26*, 8582−8588.

(22) Idota, N.; Kikuchi, A.; Kobayashi, J.; Sakai, K.; Okano, T. Modulation of Graft Architectures for Enhancing Hydrophobic Interaction of Biomolecules with Thermoresponsive Polymer-Grafted Surfaces. *Colloids Surf., B* **2012**, *99*, 95−101.

(23) Kavanagh, C. A.; Rochev, Y. A.; Gallagher, W. M.; Dawson, K. A.; Keenan, A. K. Local Drug Delivery in Restenosis Injury: Thermoresponsive co-Polymers as Potential Drug Delivery Systems. *Pharmacol. Ther.* **2004**, *102*, 1−15.

(24) Tsuda, Y.; Kikuchi, A.; Yamato, M.; Nakao, A.; Sakurai, Y.; Umezu, M.; Okano, T. The Use of Patterned Dual Thermoresponsive Surfaces for the Collective Recovery as co-Cultured Cell Sheets. *Biomaterials* **2005**, *26*, 1885−1893.

(25) Xue, B.; Gao, L.; Hou, Y.; Liu, Z.; Jiang, L. Temperature Controlled Water/Oil Wettability of a Surface Fabricated by a Block Copolymer: Application as a Dual Water/Oil on-off Switch. *Adv. Mater. (Weinheim, Ger.)* **2013**, *25*, 273−277.

(26) Braunecker, W. A.; Matyjaszewski, K. Controlled/Living Radical Polymerization: Features, Developments, and Perspectives. *Prog. Polym. Sci.* **2007**, *32*, 93−146.

(27) Hawker, C. J.; Bosman, A. W.; Harth, E. New Polymer Synthesis by Nitroxide Mediated Living Radical Polymerizations. *Chem. Rev. (Washington, DC, U.S.)* **2001**, *101*, 3661−3688.

(28) Matyjaszewski, K.; Xia, J. H. Atom Transfer Radical Polymerization. *Chem. Rev. (Washington, DC, U.S.)* **2001**, *101*, 2921−2990.

(29) Kamigaito, M.; Ando, T.; Sawamoto, M. Metal-Catalyzed Living Radical Polymerization. *Chem. Rev. (Washington, DC, U.S.)* **2001**, *101*, 3689−3746.

(30) Chiefari, J.; Chong, Y. K.; Ercole, F.; Krstina, J.; Jeffrey, J.; Le, T. P. T.; Mayadunne, R. T. A.; Meijs, G. F.; Moad, C. L.; Moad, G.; Rizzardo, E.; Thang, S. H. Living Free-Radical Polymerization by Reversible Addition-Fragmentation Chain Transfer: The RAFT Process. *Macromolecules* **1998**, *31*, 5559−5562.

(31) Percec, V.; Guliashvili, T.; Ladislaw, J. S.; Wistrand, A.; Stjerndahl, A.; Sienkowska, M. J.; Monteiro, M. J.; Sahoo, S. Ultrafast Synthesis of Ultrahigh Molar Mass Polymers by Metal-Catalyzed Living Radical Polymerization of Acrylates, Methacrylates, and Vinyl Chloride Mediated by SET at 25 °C. *J. Am. Chem. Soc.* **2006**, *128*, 14156−14165.

(32) Rosen, B. M.; Percec, V. Single-Electron Transfer and Single-Electron Transfer Degenerative Chain Transfer Living Radical Polymerization. *Chem. Rev. (Washington, DC, U.S.)* **2009**, *109*, 5069−5119.
(33) Fleischmann, S.; Rosen, B. M.; Percec, V. SET-LRP of Acrylates in Air. *J. Polym. Sci., Part A: Polym. Chem.* **2010**, *48*, 1190−1196.
(34) Zhou, Y.-N.; Zhang, Q.; Luo, Z.-H. A Light and PH Dual-Stimuli-Responsive Block Copolymer Synthesized by Copper(0)-Mediated Living Radical Polymerization: Solvatochromic, Isomerization, and "Schizophrenic" Behaviors. *Langmuir* **2014**, *30*, 1489−1499.
(35) Zhou, Y.-N.; Luo, Z.-H. Copper(0)-Mediated Reversible-Deactivation Radical Polymerization: Kinetics Insight and Experimental Study. *Macromolecules* **2014**, *47*, 6218−6229.
(36) Zhang, Q.; Wilson, P.; Li, Z.; McHale, R.; Godfrey, J.; Anastasaki, A.; Waldron, C.; Haddleton, D. M. Aqueous Copper-Mediated Living Polymerization: Exploiting Rapid Disproportionation of CuBr with Me_6TREN. *J. Am. Chem. Soc.* **2013**, *135*, 7355−7363.
(37) Samanta, S. R.; Anastasaki, A.; Waldron, C.; Haddleton, D. M.; Percec, V. SET-LRP of Methacrylates in Fluorinated Alcohols. *Polym. Chem.* **2013**, *4*, 5563−5569.
(38) Zhou, Y.-N.; Luo, Z.-H. Facile Synthesis of Gradient Copolymers *via* Semi-Batch Copper(0)-Mediated Living Radical Copolymerization at Ambient Temperature. *Polym. Chem.* **2013**, *4*, 76−84.
(39) Zhang, Q.; Li, Z.; Wilson, P.; Haddleton, D. M. Copper-Mediated Controlled Radical Polymerization under Biological Conditions: SET-LRP in Blood Serum. *Chem. Commun. (Cambridge, U.K.)* **2013**, *49*, 6608−6610.
(40) Nguyen, N. H.; Rosen, B. M.; Percec, V. SET-LRP of *N*,*N*-dimethylacrylamide and of *N*-isopropylacrylamide at 25 °C in Protic and in Dipolar Aprotic Solvents. *J. Polym. Sci., Part A: Polym. Chem.* **2010**, *48*, 1752−1763.
(41) Nguyen, N. H.; Leng, X.; Percec, V. Synthesis of Ultrahigh Molar Mass poly(2-Hydroxyethyl Methacrylate) by Single-Electron Transfer Living Radical Polymerization. *Polym. Chem.* **2013**, *4*, 2760−2766.
(42) Leng, X.; Nguyen, N. H.; van Beusekom, B.; Wilson, D. A.; Percec, V. SET-LRP of 2-Hydroxyethyl Acrylate in Protic and Dipolar Aprotic Solvents. *Polym. Chem.* **2013**, *4*, 2995−3004.
(43) Nguyen, N. H.; Kulis, J.; Sun, H.-J.; Jia, Z.; van Beusekom, B.; Levere, M. E.; Wilson, D. A.; Monteiro, M. J.; Percec, V. A Comparative Study of the SET-LRP of Oligo(Ethylene Oxide) Methyl Ether Acrylate in DMSO and in H_2O. *Polym. Chem.* **2013**, *4*, 144−155.
(44) Zhang, Q.; Collins, J.; Anastasaki, A.; Wallis, R.; Mitchell, D. A.; Becer, C. R.; Haddleton, D. M. Sequence-Controlled Multi-Block Glycopolymers to Inhibit DC-SIGN-gp120 Binding. *Angew. Chem., Int. Ed.* **2013**, *52*, 4435−4439.
(45) Zhang, Q.; Wilson, P.; Anastasaki, A.; McHale, R.; Haddleton, D. M. Synthesis and Aggregation of Double Hydrophilic Diblock Glycopolymers via Aqueous SET-LRP. *ACS Macro Lett.* **2014**, *3*, 491−495.
(46) Kashiwagi, T.; Inaba, A.; Brown, J. E.; Hatada, K.; Kitayama, T.; Masuda, E. Effects of Weak Linkages on The Thermal and Oxidative Degradation of Poly(methyl methacrylates). *Macromolecules* **1986**, *19*, 2160−21688.
(47) Bauri, K.; Roy, S. G.; Arora, S.; Dey, R. K.; Goswami, A.; Madras, G.; De, P. Thermal degradation Kinetics of Thermoresponsive Poly(N-isopropylacrylamide-*co*-*N*,*N*-dimethylacrylamide) Copolymers Prepared via RAFT Polymerization. *J. Therm. Anal. Calorim.* **2013**, *111*, 753−761.
(48) Thompson, E. V. Dependence of the Glass Transition Temperature of Poly (Methyl Methacrylate) on Tacticity and Molecular Weight. *J. Polym. Sci, Part A-2* **1966**, *4*, 199−208.
(49) Bywater, S.; Toporowski, P. M. Effcet of Stereostructure on Glass Transition Temperatures of Poly (Methyl Methacrylate). *Polymer* **1972**, *13*, 94−96.
(50) Brandrup, J.; Immergut, E. H.; Grulke,E. A. *Polymer Handbook*; Wiley: Hoboken, NJ, 1999.
(51) Biswas, C. S.; Patel, V. K.; Vishwakarma, N. K.; Tiwari, V. K.; Maiti, B.; Maiti, P.; Kamigaito, M.; Okamoto, Y.; Ray, B. Effects of Tacticity and Molecular Weight of Poly(*N*-isopropylacrylamide) on Its Glass Transition Temperature. *Macromolecules* **2011**, *44*, 5822−5824.
(52) Ito, M.; Ishizone, T. Living Anionic Polymerization of *N*-methoxymethyl-nisopropylacrylamide: Synthesis of Well-Defined Poly(*N*-isopropylacrylamide) Having Various Stereoregularity. *J. Polym. Sci., Part A: Polym. Chem.* **2006**, *44*, 4832−4845.
(53) Masci, G.; Giacomelli, L.; Crescenzi, V. Atom Transfer Radical Polymerization of *N*-isopropylacrylamide. *Macromol. Rapid Commun.* **2004**, *25*, 559−564.
(54) Xia, Y.; Yin, X.; Burke, N. A. D.; Stöver, H. D. H. Thermal Response of Narrow-Disperse Poly(*N*-isopropylacrylamide) Prepared by Atom Transfer Radical Polymerization. *Macromolecules* **2005**, *38*, 5937−5943.
(55) Sun, T.; Wang, G.; Feng, L.; Liu, B.; Ma, Y.; Jiang, L.; Zhu, D. Reversible Switching Between Superhydrophilicity and Superhydrophobicity. *Angew. Chem., Int. Ed.* **2004**, *43*, 357−360.
(56) Wenzel, R. N. Resistance of Solid Surfaces to Wetting by Water. *Ind. Eng. Chem.* **1936**, *28*, 988−994.